AIAA JOURNAL
Vol. 33, No. 2, February 1995

# Experimental Study of Flow Separation on an Oscillating Flap at Mach 2.4

Michael D. Coon* and Gary T. Chapman†
*University of California, Berkeley, Berkeley, California 94720*

**Measurements of unsteady wall pressures have been made in the turbulent boundary layer just upstream of the hinge line of an oscillating flap. The flap, which creates a highly three-dimensional compression corner flowfield, was oscillated in fully attached, crossing incipient separation, and fully separated flow regimes over a range of frequencies. It was found that a substantial lag of the pressure on the flap was produced when oscillating across the point of incipient separation. This occurred at much lower reduced frequencies than for the case of dynamic stall on an airfoil in transonic flow. The dynamic hysteresis was much less in the fully separated case and negligible in the fully attached case.**

## Nomenclature

$C_p$ = coefficient of pressure, $(P/P_{LE} - 1)/[(\gamma/2)M^2]$
$c$ = chord length of flap
$f$ = frequency of flap oscillation
$\bar{f}$ = reduced frequency, $\Theta' c/U$
$M$ = Mach number
$P$ = static pressure
$P_{LE}$ = static pressure at reference station near leading edge
$P_T$ = boundary-layer total pressure
$P_{TE}$ = total pressure at edge of boundary layer
$P_0$ = stagnation pressure
$Re_x$ = Reynolds number based on distance from leading edge, $Ux/\nu$
$Re_\delta$ = Reynolds number based on boundary-layer thickness, $U\delta/\nu$
$U$ = freestream velocity
$x$ = distance from leading edge to compression corner
$\gamma$ = ratio of specific heats
$\Theta$ = displacement angle of flap
$\Theta'$ = angular velocity of flap
$\nu$ = kinematic viscosity

## Introduction

THE understanding of fluid dynamic details of flowfields involving separated regions becomes more important as aircraft performance continues to increase. Separated flows can play a large role in the aerodynamic characteristics of high-speed vehicles and their control surfaces. An increase in the understanding of separation on three-dimensional control surfaces under stationary and dynamic boundary conditions could lead to an increase in the performance and maneuvering capability of advanced flight vehicles.

Considerable research has been done on two-dimensional fixed geometries. The work by Chapman et al.[1] and Kuehn[2,3] are examples. Work has also been done on three-dimensional separation, but again with fixed geometries. Examples are Bachalo,[4] Baroth and Holt,[5] and Settles and Bogdonoff.[6]

The dynamics of shock-induced separation on a fixed compression corner have been documented by Dolling and Murphy,[7] Dolling and Or,[8] Dolling and Brusniak,[9] Erengil and Dolling,[10] and Gramann and Dolling.[11] Dolling and Murphy[7] and Dolling and Or[8] found that the separated region in a Mach 3 flow was highly unsteady and consisted of relatively low-frequency, large-amplitude pressure fluctuations. Dolling and Brusniak[9] determined that the shock frequency was relatively independent of separation bubble length. Erengil and Dolling[10] measured dominant shock frequencies of 0.3–0.5 kHz for unswept compression corners. Gramann and Dolling[11] related the characteristic wall-pressure signal associated with separation shock turnaround to turbulence in the upstream boundary layer.

Experiments conducted by Ardonceau[12] on fixed compression ramps at Mach number 2.25 found a low-frequency component in the turbulent frequency spectrum in the vicinity of the separation bubble and suggested that it was associated with the unsteadiness of the separation bubble itself and did not affect the rest of the flow. Muck, et al.[13] examined incipient and fully separated conditions at Mach number 2.9. They documented two contributions to the fluctuating pressure signals. In the intermittent region, the unsteadiness was dominated by a large-scale "flapping" motion of the shock wave and its spanwise "rippling." In the separated region, the turbulent eddies above the recirculation zone appeared to be major contributors.

Much of the work on three-dimensional separation has been done with rather long compression ramps and, hence, long flow lengths after reattachment. Many real control surfaces may not be long compared with the separated length, and reattachment can occur very near the trailing edge, with some upstream influence from the expansion at the rear of the control surface. Also of interest in separated flow is the possibility that separation may have a subcritical bifurcation (leading to hysteresis) with flow deflection angle. This hysteresis effect may exist such that the onset and growth of separation as the flow deflection angle is increased are not the same as when the angle is decreased. Hysteresis effects could be of great importance in high-speed separated flows, particularly under dynamic boundary conditions.

The present study is the continuation of a larger study of flow separation on three-dimensional control surfaces with unsteady boundary conditions. The first part of the study, contained in Coon and Chapman[14] and Coon,[15] was a comprehensive investigation of separation on the subject control surface under steady boundary conditions. Under quasisteady conditions, the three-dimensionality and finite length effects were found to be substantial. There also appeared to be no hysteresis effects under quasisteady conditions. According to Chapman and Tobak[16] the study of the steady case was necessary as a prelude to the study with unsteady boundary conditions.

Only one previous experimental study that had examined the effect of dynamic boundary conditions on separation in a supersonic flow was found in the literature. Roberts[17] studied moving compression corners in a Mach 6.85 flow and found that the separation tended to lag the motion for a range of frequencies. However, only single-cycle motions, not oscillations, were documented.

Numerical studies by Degani and Steger[18] and Park et al.[19] examined oscillatory motion of a flap in two-dimensional cases. The

Received March 1, 1994; revision received Aug. 15, 1994; accepted for publication Aug. 17, 1994. 

*Graduate Student, Department of Mechanical Engineering; currently NRC Research Associate, NASA Ames Research Center, Moffett Field, CA 94035. Member AIAA.

†Adjunct Professor, Department of Mechanical Engineering. Member AIAA.

results of Degani and Steger were restricted to the comparison of different codes and did not discuss hysteresis effects. Park et al. identified hysteresis effects in the shock location for inviscid calculations.

The work that has been done on oscillating airfoils in transonic flows is of particular interest in examining the results of this study due to the similarity in the hysteresis effect resulting from the dynamic boundary condition. McCroskey[20] and McAlister et al.[21] are representative and document hysteresis in pressure coefficient on pitching airfoils. McCroskey provides a review of previous work and examines the case of an oscillating flap from a theoretical standpoint.

The purpose of the current study is to examine the separation phenomenon under cases of forced oscillation. The flowfield created by driving a compression corner at a known frequency and range of angles will differ from the corresponding steady-state flowfield for each angle. This work, coupled with experiments on undriven, free-to-oscillate flaps will provide information on the properties and mechanisms of unsteady separation.

## Experimental Apparatus

### Wind Tunnel

The experiments were performed in the Ames 15 × 15 cm supersonic wind tunnel in the Department of Mechanical Engineering at the University of California at Berkeley. This is a closed-cycle, continuous-flow wind tunnel with a nominal Mach number of 2.4. Both stagnation temperature and pressure are continuously adjustable. These experiments were performed at a stagnation temperature of 21°C and a stagnation pressure of $1.0 \times 10^5$ Pa (±1%).

### Model and Drive System

Figure 1 shows the geometry of the model. The model consists of a flap mechanism mounted at the rear of a splitter plate. The splitter plate is 23 cm long and spans the width of the tunnel.

The flap surface measured 7.62 × 2.54, giving it an aspect ratio of 3. These dimensions were chosen based on oil flow studies done on static wedges[14] to minimize interaction between the shock structure on the model and the tunnel sidewall boundary layers. The flap is constructed of two plates hinged by a plastic film (0.05 mm thickness) bonded to the top side to create a continuous surface. This method of construction produces an airtight corner with a radius of curvature on the order of the film thickness. The upstream plate is attached to the splitter plate, and the downstream plate is free to rotate about the hinge line. The flap is driven from below by a shaft connected to a cam drive system used to oscillate the flap over a range of frequencies from 5 to 100 Hz. An optical encoder was used to track the rotation of the cam and to synchronize the flap motion with the pressure measurements within approximately ±0.10-deg flap angle. The uncertainty in the calculation of the oscillation frequency is approximately ±8.0%.

Figure 2 is an interferogram of the entire test section and illustrates how the model affects the flowfield. A weak shock wave originating at the leading edge of the plate, due to the slight angle of attack used to suppress leading-edge separation, can be seen interacting with the thick boundary layer on the tunnel's top wall and reflecting. This shock wave hits the model just upstream of the trailing edge, but its effect on the pressure distribution on the flap was found to be negligible.[14]

### Pressure Data Acquisition System

High-frequency Kulite XT-140-25A pressure transducers were mounted on the plate and flap. These transducers have a pressure range of 0–172 kPa absolute and a natural frequency of 125 kHz. One transducer was mounted on the centerline of the plate 3.18 mm upstream of the compression corner. This position was chosen to best monitor the behavior of the shock as the flow separated. A second was mounted near the leading edge of the splitter plate to record a nominal freestream pressure used to normalize the data from the downstream transducer.

The transducers were statically calibrated before and after each tunnel run. Figure 3 shows a typical calibration data set and the resulting linear fit. Calibration data were taken both before and after each run to detect drift in transducer output that, as shown in Fig. 3, was minimal. Though the transducers were used to measure

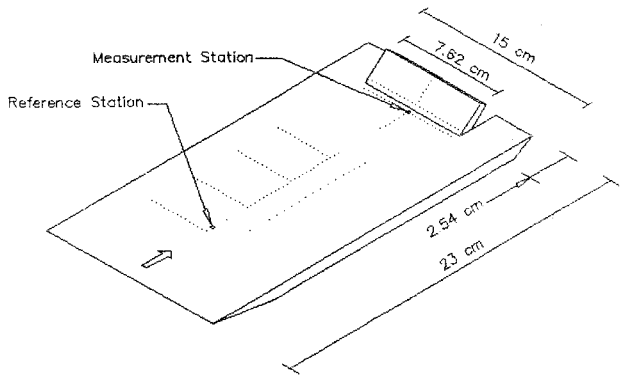


**Fig. 1 Model geometry.**

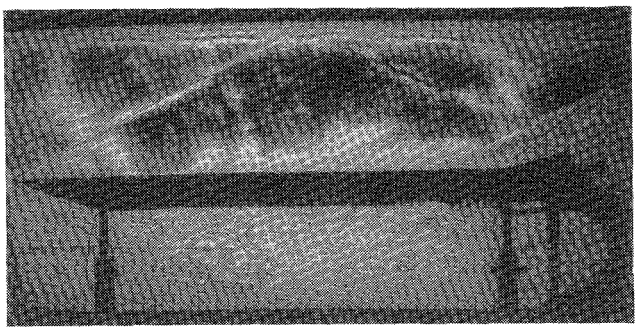

**Fig. 2 Interferogram of model.**

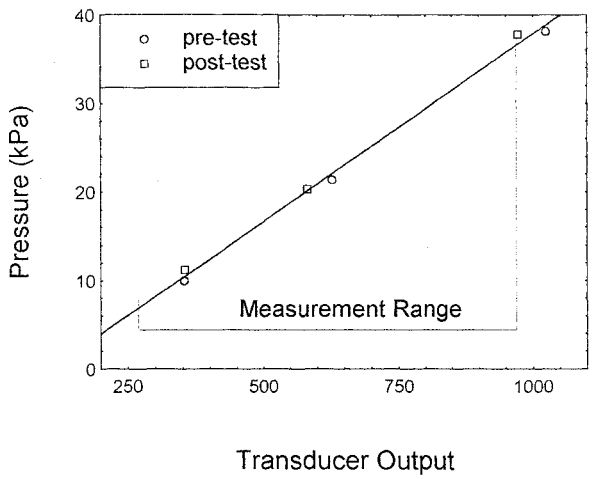


**Fig. 3 Transducer calibration.**

pressures very low in their range, the linearity of the calibrations was very good. A standard deviation from the linear fit of less than 1.0 kPa was typical. Uncertainty analysis of the calculated values resulted in an uncertainty of approximately ±20% in $C_P$ due to the combined uncertainty in $P$, $P_{LE}$, and $P_0$. However, $P_{LE}$ and $P_0$ were held constant during individual tests. Therefore, the incremental uncertainty in $C_P$ is approximately ±12%. Additionally, examination of multiple tests performed at identical conditions indicated that the repeatability was typically ±4–5% with a worst case of ±7%. Although the uncertainty of the results is high, the repeatability of the results across tests was good enough that the trends presented are considered to be significant.

A stagnation pressure probe survey was conducted to measure the boundary-layer thickness. The tip of the probe was elliptical measuring approximately 0.20 × 0.60 mm. The probe was mounted on a sting directly over the measurement station Kulite transducer and traversed in the vertical direction with the flap locked at zero deflection. The uncertainty of the pressure measurements and vertical position are approximately ±2.0% and ±0.15 mm, respectively.

A National Instruments AT-MIO-16F-5 data acquisition card and 80386 PC computer were used to sample the pressure transducers and cam position encoder. Data were taken during the oscillating test at a sampling rate of 15,000 samples per second. Measurements were taken using sampling rates as low as 3000 samples per second to demonstrate that variation of sampling rate within this range did not affect results.

**Dark Central Ground Interferometer**

Flow visualization was accomplished using a dark central ground interferometer. The theoretical background of the technique is described in detail in Anderson and Milton.[22,23] Application of the technique and operational considerations are presented in Loomis,[24] Loomis and Holt,[25] and Loomis et al.[26] Application of the technique to the current geometry during the quasisteady phase of this study are presented in Coon and Chapman.[14]

The technique can utilize either a pulse or continuous wave (CW) laser light source. The pulse laser used for this study was an Nd:YAG at 532 nm with a 20-ns pulse. The 20-ns pulse length is short enough to freeze the small-scale motions and capture the unsteady effects of the flow. The CW laser used with this system was a 5-W argon ion laser operated at 514 nm shuttered at 2.5 ms. The relatively long imaging times provided by the CW laser average any unsteady effects of the flow to allow study of the large-scale characteristics.

Details of the model and drive system design, data acquisition procedure, and optical technique can be found in Coon.[27]

## Experimental Results

**Quasisteady Results**

A boundary-layer survey was performed at the location of the measurement station indicated in Fig. 1 with the flap locked at zero deflection. The results of this survey are shown in Fig. 4. These results were used to estimate a value of 2 mm for the thickness of the undisturbed boundary layer at the compression corner. The Reynolds number for these tests, $Re_x = 2.2 \times 10^6$, can be recast as $Re_\delta = 2.2 \times 10^4$.

A series of streamwise pressure profiles along the centerline of the model were taken in a previous study. An example of these is shown in Fig. 5 taken from Coon and Chapman.[14] The flap was fixed at a particular angle for each set of measurements (i.e., steady), $Re_x = 2.2 \times 10^6$, and the boundary layer is fully turbulent. The vertical line indicates the position of the compression corner. The data point immediately upstream of the corner (indicated by an arrow) was taken at the location of the transducer used in the oscillating tests. These measurements were taken with a Baratron pressure transducer and Scanivalve indexer with an uncertainty of approximately ±2.0%.

The onset of separation is evident in Fig. 5. As the flap angle is increased, the pressure rise begins to feed upstream from the compression corner. Separated flow is characterized by a sharp rise in pressure upstream of the compression corner that levels off in a plateau over the separated region and increases again at reattachment. The angle for incipient separation in these tests is slightly less than 20 deg.

To establish a baseline for the oscillating experiments, measurements were taken under quasisteady conditions over the range of test angles. This case is designated quasisteady rather than steady because the flap was moved slowly ($\Theta' < 0.02$ rad/s compared with $\Theta' > 2.0$ rad/s for the oscillating tests) to each successive position and then held fixed while measurements were recorded at the transducer location indicated on Fig. 1. The results of the quasisteady test are shown in Fig. 6. For low angles, the pressure signal remains small and constant but above the zero deflection value. This is probably due to pressure feeding forward in the boundary layer. The pressure increases slightly as incipient separation is neared.

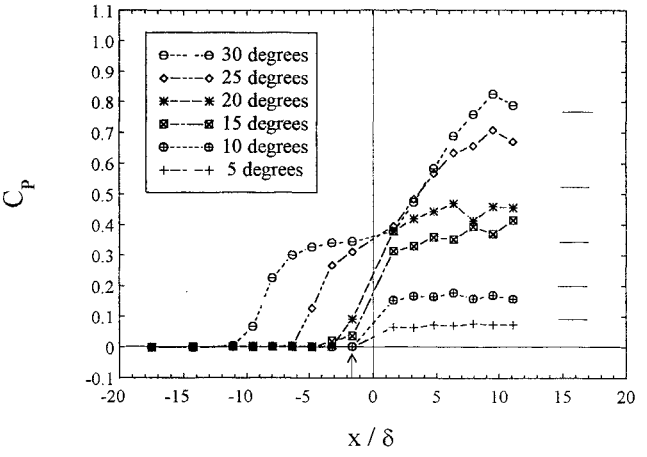


**Fig. 5 Streamwise pressure profile, $Re = 2.2 \times 10^6$.**

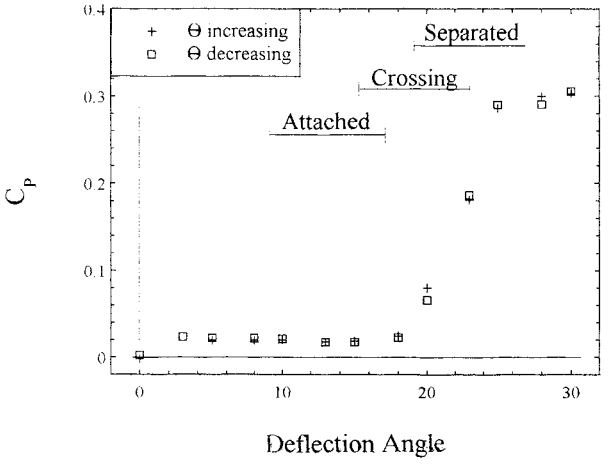


**Fig. 6a $C_p$ under quasisteady conditions.**

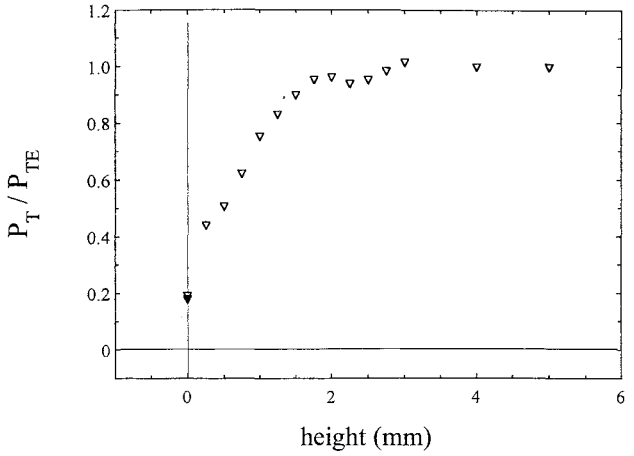


**Fig. 4 Boundary-layer profile, $Re = 2.2 \times 10^6$.**

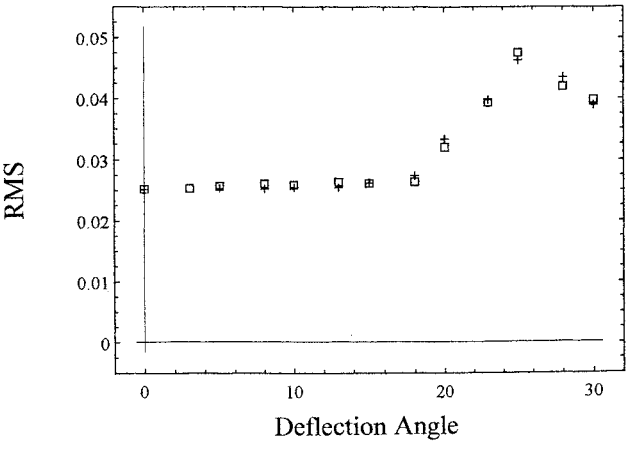


**Fig. 6b rms of $C_p$ under quasisteady conditions.**

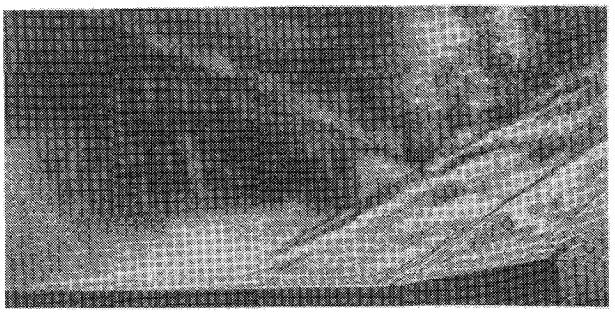

Fig. 7a Interferogram, deflection angle 10 deg.

Fig. 7b Interferogram, deflection angle 30 deg.

The pressure value jumps dramatically as the shock wave moves upstream of the transducer and reaches a near constant value under the separated region. The bars on the figure indicate the range of angles over which the oscillating tests were performed. Figure 6b shows the rms of the pressure coefficient. Note the jump in the rms of the pressure signal when the shock wave crosses the transducer and the decrease as the shock moves upstream.

Interferograms, taken from Coon and Chapman,[14] for $Re_x = 2.2 \times 10^6$ and two flap deflection angles (10 and 30 deg) are illustrated in Fig. 7. This figure presents interferograms taken with the Nd:YAG pulse laser under quasisteady conditions. In the 10-deg case, the boundary layer is attached. Comparison of this photograph with others taken with the CW laser indicated the relative steadiness of the flowfield. In the 30-deg case, the boundary layer is separated far upstream of the compression corner. In this case, comparison with CW laser results showed that both the shock wave and the flow behind the shock wave are highly unsteady. In both of these photographs, a weak shock is evident on the splitter plate upstream of the interaction. This shock originates from the joint between the flap assembly and the splitter plate. Pressure profile taken under steady conditions indicated no response to this shock.

**Oscillating Flap Results**

Figures 8–10 illustrate pressure coefficients for data taken during oscillating conditions and phase-locked to overlay the cycles. Figure 8 illustrates measurements taken in the fully attached regime oscillating from 9 to 17 deg. Figure 9 presents data taken during oscillations from 15–23 deg, which crosses the point of incipient separation and forces the flow to separate and reattach during each cycle. Figure 10 shows oscillations of 19–27 deg during which the flow is fully separated. The periodic nature of the data in each case is evident. The profile of the cycle also becomes broader as the flow progresses from fully attached to fully separated, reflecting higher pressure levels over more of the cycle.

Figures 11–17 present $C_p$ and rms of $C_p$ results plotted vs flap deflection angle. In these figures, each cycle had been folded about its centerline, overlaying the angle increasing and the angle decreasing data to illustrate the lack of symmetry. The square data points indicate data taken with flap angle increasing and the crosses indicate flap angle decreasing. The solid line on each graph is a curvefit of the quasisteady measurements through the corresponding angles.

Figures 11 and 12 illustrate oscillation over 9 to 17 deg. These angles fall in a range at which the quasisteady results were fully

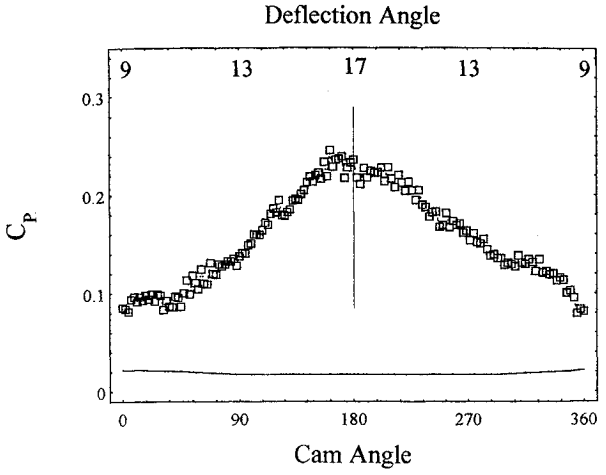


Fig. 8 $C_p$, fully attached cycle, $\bar{f} = 3.40 \times 10^{-4}$.

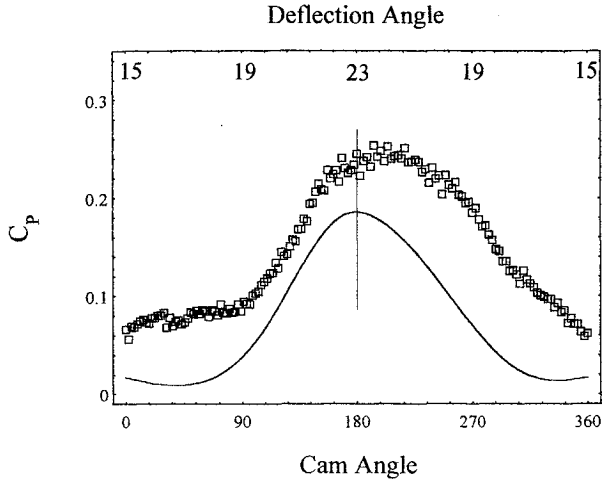


Fig. 9 $C_p$, crossing separation cycle, $\bar{f} = 3.25 \times 10^{-4}$.

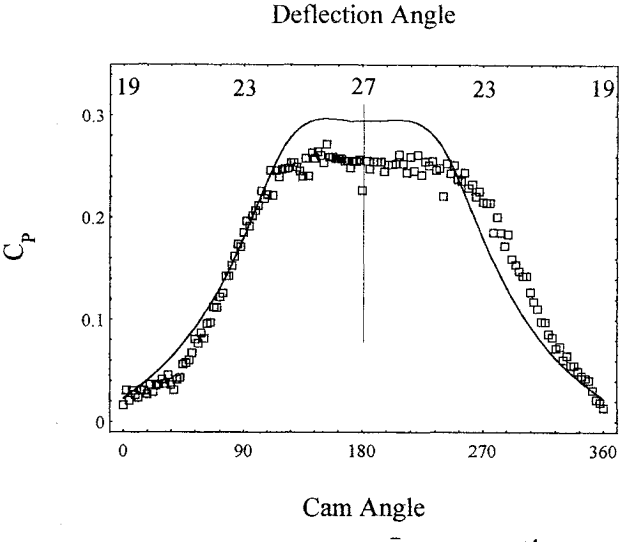


Fig. 10 $C_p$, fully separated cycle, $\bar{f} = 3.22 \times 10^{-4}$.

attached. In the quasisteady case, the pressure varied only slightly as indicated by the nearly flat solid line. The frequencies shown in Figs. 11 and 12 are $f = 9.1$ and 26.7 Hz, respectively.

The coefficient of pressure values for oscillation in the fully attached range lie entirely above the quasisteady results, representing a thickening of the boundary layer in the oscillating case. The results also show an increase at the high end of the oscillation range. This indicates that the pressure rise caused by the compression corner

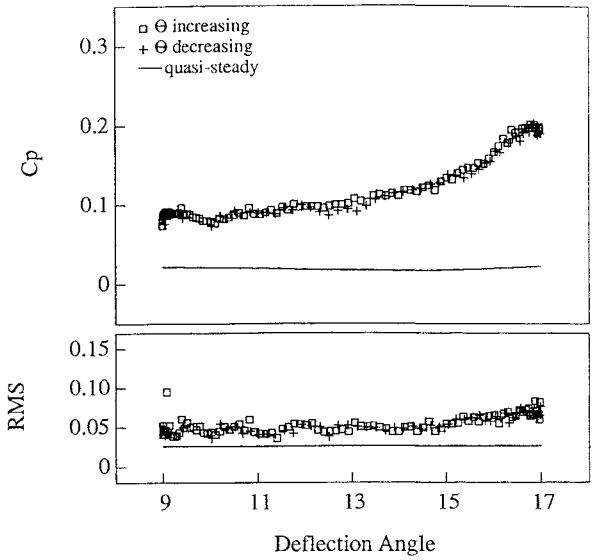


Fig. 11 $C_p$ and rms of $C_p$, fully attached cycle, $\bar{f} = 1.16 \times 10^{-4}$.

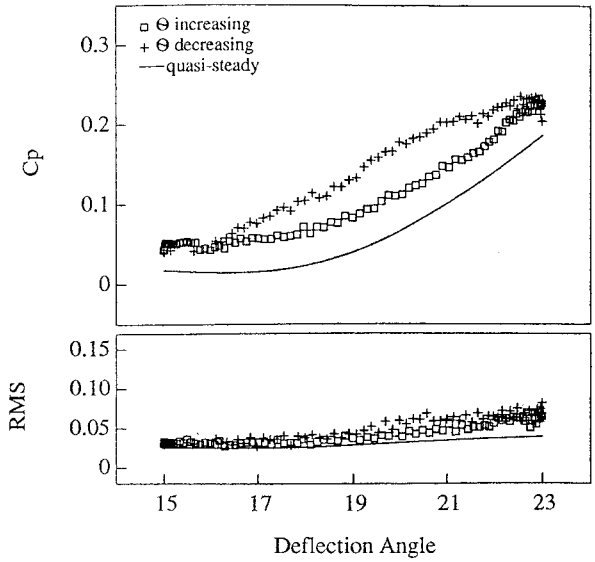


Fig. 14 $C_p$ and rms of $C_p$, crossing separation cycle, $\bar{f} = 2.25 \times 10^{-4}$.

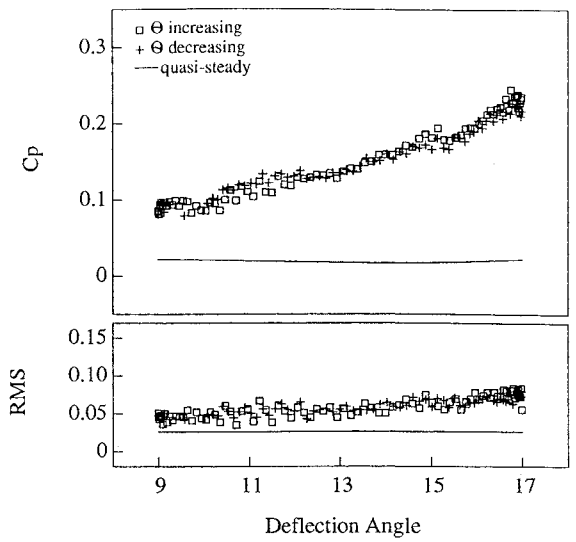


Fig. 12 $C_p$ and rms of $C_p$, fully attached cycle, $\bar{f} = 3.40 \times 10^{-4}$.

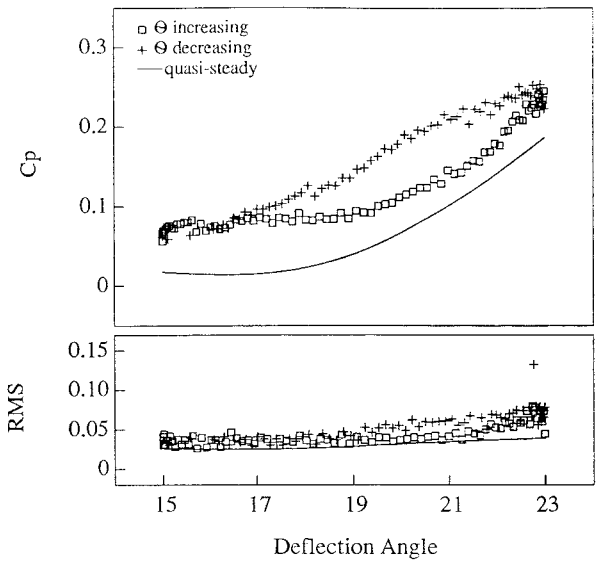


Fig. 15 $C_p$ and rms of $C_p$, crossing separation cycle, $\bar{f} = 3.25 \times 10^{-4}$.

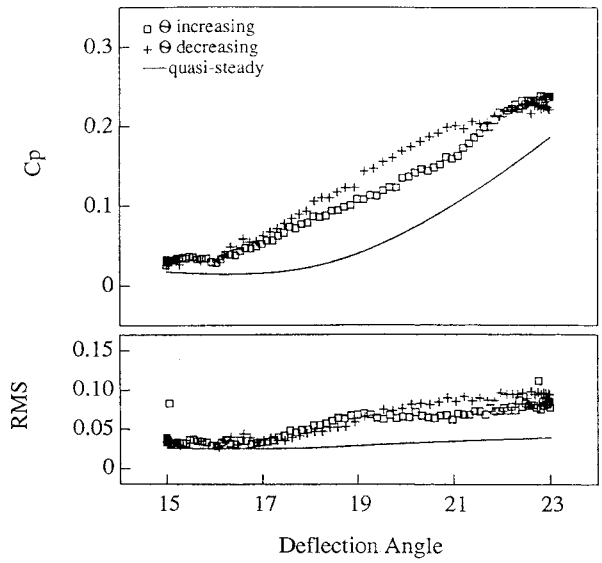


Fig. 13 $C_p$ and rms of $C_p$, crossing separation cycle, $\bar{f} = 1.04 \times 10^{-4}$.

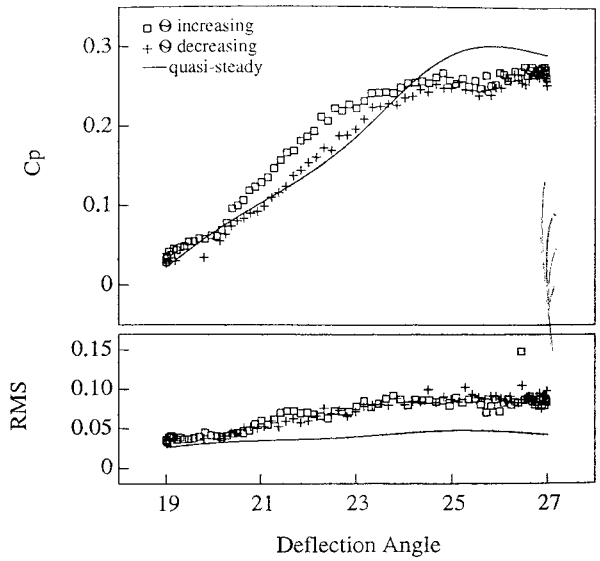


Fig. 16 $C_p$ and rms of $C_p$, fully separated cycle, $\bar{f} = 1.44 \times 10^{-4}$.

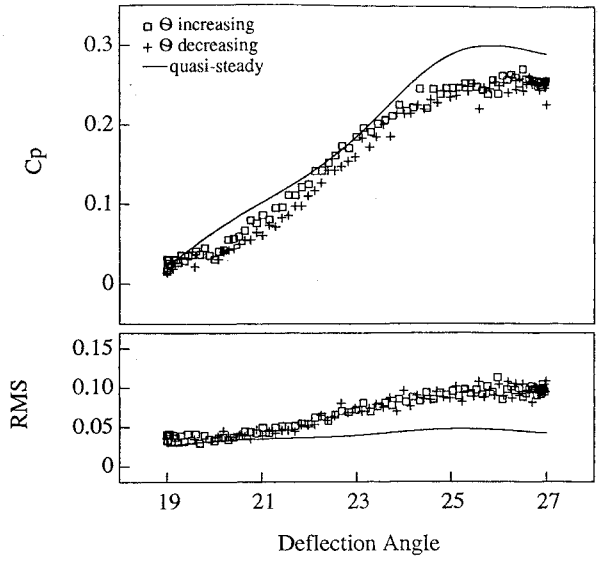


**Fig. 17** $C_p$ **and rms of** $C_p$**, fully separated cycle,** $\bar{f} = 3.22 \times 10^{-4}$.

is penetrating further upstream in the thickened boundary layer. However, the coincidence of the data for flap angle increasing and decreasing and the fairly constant rms values suggest that the boundary layer does not separate.

Figures 13–15 display data taken while oscillating the flap over the range 15–23 deg for a range of frequencies. This range of angles brackets the angle for the onset of separation, which occurred at approximately 20 deg in the quasisteady tests. Figures 13–15 represent nominal frequencies of $f = 8.2$, 17.7, and 25.5 Hz, respectively.

Each of the pressure coefficient plots shows a hysteresis indicating a lag in the pressure signal with respect to the flap angle. This is a result of the boundary layer remaining separated as the flap angle falls below the value of incipient separation. As the flap angle decreases, the separated region does not shrink as quickly as it grew with flap angle increasing. The lag effect tends to increase with an increase in oscillation frequency. This effect is similar to dynamic stall on an airfoil;[20–21] however, the reduced frequency at which the effect becomes noticeable is much lower in this case. The amount of hysteresis at these low reduced frequencies suggests that the time scales associated with onset and disappearance of separation are long compared with inviscid time scales. Overall, the values of $C_p$ lie above those measured in the quasisteady tests, representing a general thickening of the boundary layer due to the oscillating flap.

The various rms of $C_p$ values associated with the oscillation across incipient separation show a increase at higher angles consistent with the quasisteady results, indicating that the separation point moves upstream of the transducer. The value of the rms at the highest angles decreases as the frequency of oscillation increases. The causes of this effect are uncertain.

Figures 16 and 17 represent data taken in oscillations of flap angle from 19 to 27 deg. The low end of this range is the angle at which the quasisteady results showed incipient separation. The frequencies shown are $f = 11.3$ and 25.3 Hz, respectively. The pressure values are consistent with the quasisteady results, and the values suggest that the boundary layer remains separated throughout the range of angles. There is a dynamic hysteresis loop, but it is much smaller than that found when oscillating across the angle of incipient separation. The rms values show an increase at higher flap angles as suggested by the quasisteady data.

It is significant that the pressure measurements in the fully attached regime are higher than the quasisteady measurements for every case, whereas the fully separated results corresponded well with the quasisteady measurements. The results taken in the midrange crossing separation lie slightly above the quasisteady results, but less so than the fully attached cases. The shape of the fully attached cycle, as shown in Fig. 8, is characteristic of the profile of the pressure change on the flap downstream of the shock. It is possible that the pressure on the flap surface is feeding upstream through the boundary layer and that the mechanism that dynamically couples the two positions has a time scale too slow to allow relaxation to the quasisteady conditions. However, once separation occurs, the spanwise velocity component in the three-dimensional separation rapidly ventilates the upstream region, hence providing a mechanism for relaxation to the quasisteady level.

Further analysis was performed on the pressure data. Power spectrum analysis revealed little information. The power spectrum of the oscillating data differed from the quasisteady data only with the presence of a low-frequency component corresponding to the driving frequency. Embedding techniques were performed, resulting in limit cycle loops corresponding to the periodic signal expected. No fine structure in the embedding diagrams was evident due to the amount of noise in the data. In both of these cases, further analysis was hampered by the low signal-to-noise ratio of the data resulting from operation of the pressure transducers near the bottom of their dynamic range.

## Conclusions

An experimental investigation has been conducted of the flow separation upstream of an oscillating flap. Oscillations were performed over a range of flap angles representing fully attached, crossing incipient separation, and fully separated flow regimes. A variety of frequencies were examined. Static pressure was measured at a position slightly upstream of the compression corner and compared with quasisteady results.

Pressure measurements during oscillation of the flap in the fully attached range were higher than quasisteady results. The data also showed an increase at higher angles not displayed in the quasisteady data. The oscillation of the flap appears to cause a thickening of the upstream boundary layer that increases the effect of the adverse pressure gradient.

Oscillations across the angle of incipient separation resulted in a hysteresis effect, indicating a lag in the pressure response to flap angle. Reattachment of the boundary layer appears to be delayed as the flap angle decreases. In addition, the pressure values were consistently higher than the quasisteady measurements as a result of the thickened boundary layer.

In the fully separated regime, the results were closer to the quasisteady measurements, and very little hysteresis effects were seen.

It is hypothesized that the time scales associated with attached flow are longer than those associated with separated flow and that the spanwise flow in the three-dimensional separation zone is responsible for this difference. A more detailed study using other types of instrumentation such as thin film gauges or multiple pressure transducers is required to verify this.

## References

[1]Chapman, D. R., Kuehn, D. M., and Larson, H. K., "Investigation of Separated Flows in Supersonic and Subsonic Streams with Emphasis on the Effects of Transition," NACA TR 1356, 1958.

[2]Kuehn, D. M., "Turbulent Boundary-Layer Separation Induced by Flares on Cylinders at Zero Angle of Attack," NASA TR R-117, 1961.

[3]Kuehn, D. M., "Laminar Boundary-Layer Separation Induced by Flares on Cylinders at Zero Angle of Attack," NASA TR R-146, 1962.

[4]Bachalo, W. D., "Experiments on Supersonic Boundary-Layer Separation in Three Dimensions," *Journal of Applied Mechanics*, Vol. 42, No. 2, 1975, pp. 289–294.

[5]Baroth, E. C., and Holt, M., "Investigation of Supersonic Separated Flow in a Compression Corner by Laser Doppler Anemometry," *Experiments in Fluids*, Vol. 1, 1983, pp. 195–203.

[6]Settles, G. S., and Bogdonoff, S. M., "Scaling of Two- and Three-Dimensional Shock/Turbulent Boundary Layer Interactions at Compression Corners," *AIAA Journal*, Vol. 20, No. 6, 1982, pp. 782–789.

[7]Dolling, D. S., and Murphy, M. T., "Unsteadiness of the Separation Shock Wave Structure in a Supersonic Compression Ramp Flowfield," *AIAA Journal*, Vol. 21, No. 12, 1983, pp. 1628–1634.

[8]Dolling, D. S., and Or, C. T., "Unsteadiness of the Shock Wave Structure in Attached and Separated Compression Ramp Flows," *Experiments in Fluids*, Vol. 3, 1985, pp. 24–32.

[9]Dolling, D. S., and Brusniak, L., "Separation Shock Motion in Fin, Cylinder, and Compression Ramp-Induced Turbulent Interactions," *AIAA Journal*, Vol. 27, No. 6, 1989, pp. 734–742.

[10]Erengil, M. S., and Dolling, D. S., "Effects of Sweepback on Unsteady Separation in Mach 5 Compression Ramp Interactions," AIAA Paper 92-0430, Jan. 1992.

[11]Gramann, R. A., and Dolling, D. S., "A Preliminary Study of Turbulent Structures Associated with Unsteady Separation Shock Motion in a Mach 5 Compression Ramp Interaction," AIAA Paper 92-0744, Jan. 1992.

[12]Ardonceau, P. L., "The Structure of Turbulence in a Supersonic Shock-Wave/Boundary-Layer Interaction," *AIAA Journal*, Vol. 22, No. 9, 1984, pp. 1254–1262.

[13]Muck, K., Andreopoulos, J., and Dussuage, J., "Unsteady Nature of Shock-Wave/Turbulent Boundary-Layer Interaction," *AIAA Journal*, Vol. 26, No. 2, 1988, pp. 179–187.

[14]Coon, M. D., and Chapman, G. T., "A Study of Flow Separation on an Aspect Ratio Three Flap at Mach Number 2.4," AIAA Paper 91-1620, June 1991.

[15]Coon, M. D., "A Study of Flow Separation on an Aspect Ratio Three Flap at Mach Number 2.4," Master's Report, Univ. of California at Berkeley, Berkeley, CA, 1991.

[16]Chapman, G. T., and Tobak, M., "Bifurcations in Unsteady Aerodynamics—Implications for Testing," *Proceedings of the Workshop on Unsteady Separated Flows*, U.S. Air Force Academy, Colorado Springs, CO, July 1987.

[17]Roberts, T. P., "Dynamic Effects of Hypersonic Separated Flow," Ph.D. Thesis, Univ. of Southampton, Southampton, England, UK, 1989.

[18]Degani, D., and Steger, J., "Comparison Between Navier-Stokes and Thin-Layer Computations for Separated Supersonic Flow," *AIAA Journal*, Vol. 21, No. 11, 1983, pp. 1604, 1605.

[19]Park, S. O., Chung, Y. M., and Sung, H. J., "Numerical Study of Unsteady Supersonic Compression Ramp Flows," *AIAA Journal*, Vol. 32, No. 1, 1994, pp. 216–218.

[20]McCroskey, W. J., "Unsteady Airfoils," *Annual Review of Fluid Mechanics*, Vol. 14, 1982, pp. 285–311.

[21]McAlister, K. W., Carr, L. W., and McCroskey, W. J., "Dynamic Stall Experiments on the NACA 0012 Airfoil," NASA TP-1100, Jan. 1978.

[22]Anderson, R. C., and Milton, J. E., "A Large Aperture Inexpensive Interferometer for Routine Flow Measurements," *Proceedings of the International Congress on Instrumentation in Aerospace Simulation Facilities*, (Gottingen, West Germany), Sept. 1989.

[23]Anderson, R. C., and Milton, J. E., "Conversion of Schlieren Systems to High Speed Interferometers," 19th International Congress on High Speed Photography and Photonics, Cambridge, England, UK, Sept. 1990.

[24]Loomis, M. P., "Interferometric Investigation of Supersonic Flow Fields with Shock-Shock Interactions," Ph.D. Thesis, Univ. of California, Berkeley, CA, May 1990.

[25]Loomis, M. P., and Holt, M., "Interferometric Investigation of Supersonic Flow Fields with Shock-Shock Interactions," Fifth International Symposium on Application of Laser Techniques to Fluid Mechanics, Lisbon, Portugal, July 1990.

[26]Loomis, M. P., Holt, M., Chapman, G. T., and Coon, M., "Application of Dark Central Ground Interferometry," AIAA Paper 91-0565, Jan. 1991.

[27]Coon, M. D., "A Study of Flow Separation on an Oscillating Flap at Mach Number 2.4," Ph.D. Thesis, Univ. of California, Berkeley, CA, May 1993.